



## Research paper

# Spontaneous termination of reentrant activity under myocardial acute ischemia: Role of cellular conductivity and its relation to ischemic heterogeneities

Edda Boccia<sup>a,\*</sup>, Ulrich Parlitz<sup>a,b</sup>, Stefan Luther<sup>a,b,c</sup><sup>a</sup> Max Planck Institute for Dynamics and Self-Organization, Am Fassberg 17, Göttingen D-37077, Germany<sup>b</sup> Institute for Nonlinear Dynamics, Georg-August-Universität, Friedrich-Hund-Platz 1, Göttingen D-37077, Germany<sup>c</sup> Department of Pharmacology, University Medical Center, Robert-Koch-Str.40, Göttingen D-37075, Germany

## ARTICLE INFO

## Article history:

Received 14 September 2016

Accepted 5 December 2016

Available online 6 December 2016

## MSC:

00-01

99-00

## Keywords:

Cardiac arrhythmias

Spiral waves

Bidomain Luo and Rudy I model

Myocardial acute ischemia

## ABSTRACT

The relation between reentrant activity and occurrence of cardiac arrhythmias still is a topic of intensive investigation. Reentries are strictly related to and enhanced by the complex structure of cardiac tissue, characterized by multi-sized electrophysiological and spatial heterogeneities. However, the structure and the function of the tissue can sometimes also promote phenomena of spontaneous termination of waves. The role played by the tissue in this scenario is not well understood and yet under investigation. In this study, we implemented a bidomain formulation of the phase I of the Luo and Rudy action potential model in 2D under ischemic conditions. We investigate how the size of ischemic heterogeneities and tissue conduction properties may affect the system dynamics and drive it towards maintenance of reentrant activity or quiescence.

The main findings show that: (a) for the stability of the waves, changes of conductivity in the intracellular space are more critical than alterations in the extracellular space; (b) the maintenance or the self-termination of pinned spirals is strongly dependent not only on the size of the heterogeneities but also on the degree of intracellular anisotropy.

These findings confirm and extend results obtained from previous investigations. In addition, since experimental values of conductivity tensors reported in the literature are not consistent, an overview of possible scenarios arising from a broader range of assumed anisotropy values is provided in relation to different sizes of ischemic heterogeneities. In this perspective, simulations are shown to compare the impact of different degrees of tissue anisotropy on wave dynamics.

© 2016 The Authors. Published by Elsevier B.V.

This is an open access article under the CC BY license

[\(http://creativecommons.org/licenses/by/4.0/\)](http://creativecommons.org/licenses/by/4.0/).

## 1. Introduction

There is strong evidence in literature suggesting that reentrant activity is one of the main causes of the occurrence of cardiac arrhythmias [1–3], among which some (like ventricular tachycardia (VT) and ventricular fibrillation (VF)) can be seriously life threatening if not properly treated and can lead to sudden cardiac death [4,5]. Reentries are highly promoted

\* Corresponding author.

E-mail addresses: [edda.boccia@ds.mpg.de](mailto:edda.boccia@ds.mpg.de) (E. Boccia), [ulrich.parlitz@ds.mpg.de](mailto:ulrich.parlitz@ds.mpg.de) (U. Parlitz), [stefan.luther@ds.mpg.de](mailto:stefan.luther@ds.mpg.de) (S. Luther).

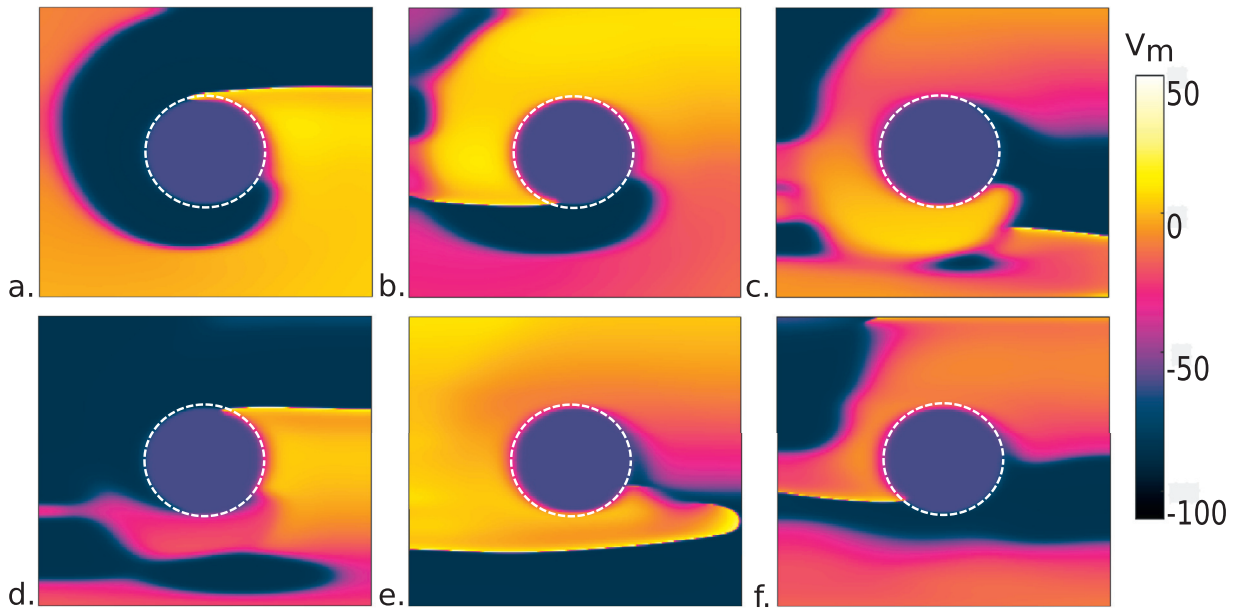


**Fig. 1.** Snapshots showing maintenance of a spiral wave pinned to the ischemic heterogeneity having a radius of 0.67 cm, highlighted by the white dashed circle. Simulations were run using a bidomain formulation of the phase I of the Luo and Rudy action potential model. The 2D domain was represented by a  $3.67 \times 3.67 \text{ cm}^2$  sheet of heterogeneous and anisotropic cardiac tissue, in which fibers were supposed to be aligned along the  $x$ -axis. The color bar indicates the membrane potential  $V_m$  in mV: (a) time = 70 ms; (b) time = 200 ms; (c) time = 350 ms; (d) time = 580 ms; (e) time = 700 ms; (f) time = 980 ms. (For interpretation of the references to color in this figure, the reader is referred to the web version of this article.)

by the complex myocardial structure, in which electrophysiological and spatial multi-sized heterogeneities represent a critical substrate. Heterogeneities can be intrinsic or can be exacerbated after the occurrence of specific diseases [6]: in both cases they affect the properties of the tissue causing reduced conduction velocity, prolonged refractory period, discordant repolarization alternans or repolarization gradients [7–15].

The concept of spiral waves was introduced in 1946 [16] with respect to reentries anchored to anatomical features of the tissue and then extended to refer to waves circulating around “functional” obstacles, i.e. not anatomical, called the core of the spiral. Once a reentry develops in the tissue, it can remain stable showing VT or it can break up into multiple wavelets, i.e. degenerating into VF. In the latter case two types of VF have been hypothesized and experimentally validated in animal models: the “mother rotor” and the “multiple wavelets” [17]: in the first case, pre-existing heterogeneities play an important role in causing conduction block of waves propagating from a stable rotor and are responsible for the development of multiple wavelets during fibrillation [18]; in the second case, instead, the fibrillation and the development of multiple waves is sustained by continuous waves break up due to dynamical instabilities [19].

In 1914 Garrey et al. [20] introduced the concept of the “critical mass hypothesis”, according to which formation and maintenance of cardiac arrhythmias is strongly affected by the size and form of the tissue. Beyond shock-induced termination [21], under certain conditions arrhythmias may also terminate spontaneously into quiescence: this may happen when the wavelength (and the refractory period) are increased in some regions of the tissue, causing a reduction of tissue size and, as a consequence, termination of reentrant activity. Beyond wavelength [22], other features have been shown by previous studies to play a role in the interactions between wave and obstacles: among them, dynamical instabilities (such as chaos) [7], size of anatomical and functional obstacles [23,24], excitability and curvature of the obstacles [25], thickness, shape and geometry of the tissue [20,24].

In this paper the effects exerted by both geometry and electrophysiological properties of the tissue on maintenance and self-termination of reentrant waves are discussed. In this perspective, we implemented a bidomain formulation of the phase I of the Luo and Rudy action potential model [26] under conditions of acute ischemia, starting from initial conditions in which reentrant waves are pinned to ischemic heterogeneities. The roles played by the size of the heterogeneities and by the change of conduction properties in the tissue are analyzed, showing interesting examples of how these parameters and their combination can highly influence wave dynamics pushing the system to persistence of reentrant activity or quiescence.

## 2. Maintenance and spontaneous termination of cardiac arrhythmias

Figs. 1(a)–(f) and Fig. 2(a)–(f) show snapshots from simulations of maintenance and spontaneous termination of reentrant activity, respectively. A spiral wave is pinned to an ischemic region with radius of 0.67 cm. In both cases the dynamics of the waves develops under conditions of acute ischemia and the size of the heterogeneity stays constant, but due to

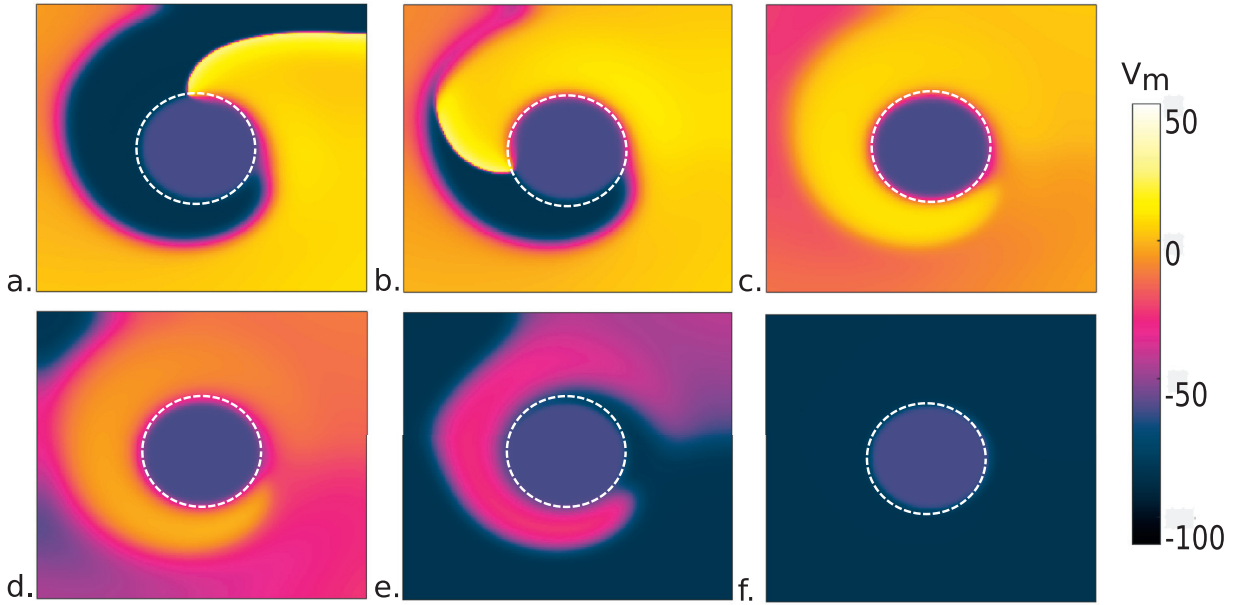


**Fig. 2.** Snapshots showing self-termination of the spiral pinned to the ischemic heterogeneity having a radius of 0.67 cm, highlighted by the white dashed circle. Simulations were run using a bidomain formulation of the phase I of the Luo and Rudy action potential model. The 2D domain was represented by a  $3.67 \times 3.67$  cm<sup>2</sup> sheet of heterogeneous and anisotropic cardiac tissue, in which fibers were supposed to be aligned along the  $x$ -axis. The color bar indicates the membrane potential  $V_m$  in mV: (a) time = 40 ms; (b) time = 70 ms; (c) time = 150 ms; (d) time = 250 ms; (e) time = 350 ms; (f) time = 500 ms. (For interpretation of the references to color in this figure, the reader is referred to the web version of this article.)

a change in the tissue conduction properties (in particular in its degree of anisotropy) the spiral behavior follows two opposite directions. In case of maintenance the wave slightly changes its shape but never detaches from the heterogeneity (see Fig. 1(c)–(f)). In case of termination the system slowly evolves towards quiescence due to a spiral tip-tail collision (see Fig. 2(c)–(f)). Additional details on the implemented mathematical model and on the simulated domain, together with a comprehensive discussion on the possible reasons for the difference between the two observed outcomes will be given further in the text.

### 3. Methods

#### 3.1. Mathematical model

The tissue is represented by a bidomain model. The transmembrane potential  $V_m$  and the extracellular potential  $V_e$  are described by the following partial differential equations:

$$\nabla \cdot (\sigma_e + \sigma_i) \nabla V_e = \nabla \cdot \sigma_i \nabla V_m \quad (1)$$

$$\nabla \cdot \sigma_e \nabla V_e = \beta \left[ C_m \frac{\partial V_m}{\partial t} + I_{ion} \right] \quad (2)$$

where  $\beta$  is the ratio of membrane surface area to tissue volume ( $0.2 \text{ cm}^{-1}$ ),  $C_m$  is the membrane capacitance per unit area ( $1 \mu\text{Fcm}^{-2}$ ),  $\sigma_e$  and  $\sigma_i$  are the extracellular and intracellular conductivity tensors, and  $I_{ion}$  is the sum of transmembrane ionic currents, described by the local ionic model.

For the latter, the phase I of the Luo and Rudy action potential model was chosen [26]. In order to simulate the electrophysiological and structural remodeling occurring in myocardial tissue due to the lack of blood flow, the ionic model and the conductivity tensors in the heterogeneity were modified accordingly. The ischemic area was not treated as an insulator, but as a region with reduced conduction properties. For these reasons, conditions of hyperkalemia and acidosis arising at the cellular level were modeled: hyperkalemia was obtained by increasing the extracellular potassium concentration,  $[K^+]_o$ , from 5.4 to 14 mmol/L [27]; acidosis exerted its effects on the sodium and L-type calcium channel specific conductances,  $g_{Na}$  and  $g_{Ca}$  (both chosen according to Luo et al. [26]), respectively, which were both reduced by 25% [28]. To reproduce the changes in intracellular and extracellular conductivities, experimental data provided by Kléber et al. [29] were adopted. After the arrest of coronary flow, there is an immediate increase in extracellular resistance of approximately 30%, connected to a drop in perfusion pressure and probably due to the diminution of intravascular volume. Later, a second gradual increase

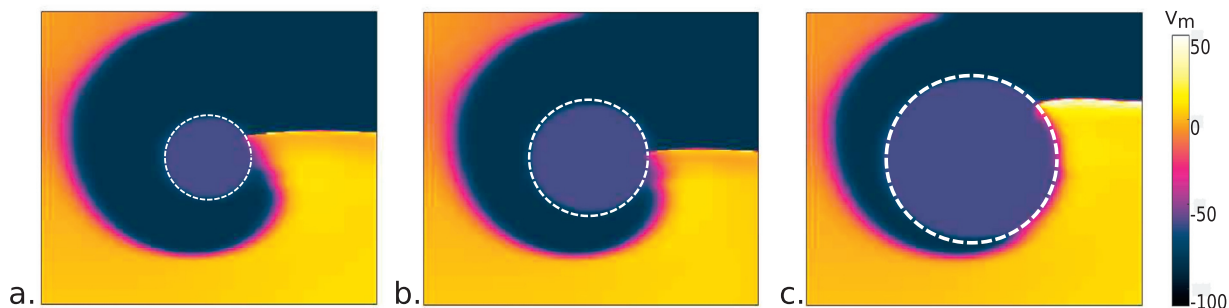


**Fig. 3.** Initial conditions in which heterogeneities have different radii  $r_{IZ}$ . The ischemic heterogeneity IZ is highlighted by the white dashed circle: (a)  $r_{IZ} = 0.3$  cm; (b)  $r_{IZ} = 0.67$  cm; (c)  $r_{IZ} = 1$  cm. The color bar indicates the membrane potential  $V_m$  in mV. (For interpretation of the references to color in this figure, the reader is referred to the web version of this article.)

up to 80% occurs after 20 min. The intracellular resistance is supposed to remain constant in the first 10–12 min, after that there is a steep increment due to progressing cellular uncoupling and a breakdown of cellular homeostasis. Taking these phenomena into account, bidomain conductivities in the ischemic heterogeneity were reduced by 40% in the extracellular domain and by 50% in the intracellular domain. Anisotropic properties were also introduced and myocardial fibers were modeled as straight and directed along the  $x$ -direction. Both spaces had different conductivities in the directions parallel (longitudinal) and perpendicular (transverse) to fibers, with a different degree of anisotropy: due to this latter feature, many interesting phenomena are known to arise in the intracellular and interstitial spaces [30,31].

### 3.2. Simulated domain

Figs. 3(a)–(c) show three 2D sheets of tissue (3.67 cm diameter) used as initial conditions for simulations. Each domain has a central circular heterogeneity (highlighted by the white dashed circle), representing the region in which acute ischemia had developed. The radius of the ischemic zone ( $r_{IZ}$ ) ranged from 0.3 cm to 1 cm. For each domain, initial conditions consisted of a single spiral pinned to the ischemic zone (IZ) with the aim to investigate the role played by both anisotropy ratios and IZ dimensions in dynamical stability of waves.

In the first set of simulations, the dynamical evolution of the spiral was explored for each size of the heterogeneity, in dependence on intracellular and extracellular conductivities. Bidomain conductivities have been measured experimentally [32–36], but data are inconsistent and therefore no consensus exists regarding the accurate values of these parameters and their anisotropy ratios. The anisotropy ratio is defined as the ratio between the longitudinal ( $\sigma_L$ ) and transversal ( $\sigma_T$ ) conductivities [37].

Our simulations refer to experimental values introduced by Clerc et al. [32], who report anisotropy ratios of approximately 9 and 2.6 in the intracellular and extracellular domains, respectively. Taking these values into account, anisotropy ratios were changed in both healthy and ischemic tissues, tuning transversal conductivities at different percentages of the corresponding longitudinal ones. In both the intracellular and extracellular domains, a wide range of parameters was spanned, from  $\sigma_T = 10\% \sigma_L$  to  $\sigma_T = \sigma_L$ : with this approach many possible conditions were addressed from high to low anisotropy, until isotropy was reached. In addition, a series of physiological conditions was simulated: a change in intracellular conductivities reflect a change in intercellular coupling via gap-junctions and, in the worse case, it can alter action potential conduction velocity in ways that contribute significantly to the onset of reentrant arrhythmias after myocardial ischemia and infarction [38]. On the other hand, alterations of the extracellular conductivities can lead to osmotic swelling: abnormal values induce cellular mechanisms (i.e. ionic pumps) dysfunctions and, as result, anomalous ionic and water concentrations [39].

In the second set of simulations, the size of the heterogeneity was introduced as a variable and its effects were directly compared to the intracellular anisotropy ratio, which from the previous analysis resulted to be the most significant parameter, as it will be described in more detail in the next section. Fixing the extracellular conductivities to their experimental values [32], the spiral evolution (maintenance or self-termination) was investigated with respect to different dimensions of IZ and different degrees of anisotropy. It has already been shown by previous studies that tissue geometry can play a role in spontaneous termination of reentries [20,24]: this method allowed to make a direct comparison between obstacle size effects and the wave propagation directionality imposed by fibers.

All simulations use no-flux boundary conditions, a space step  $\Delta x = \Delta y = 0.016$  cm and a time step of 0.01 ms in the bidomain model and 0.05 ms in the local model.

## 4. Numerical simulations and results

Results from simulations with the initial conditions shown in Fig. 3 are reported in Fig. 4. In each set of simulations, different degrees of anisotropy are imposed by tuning transversal conductivities at different percentages of the respective

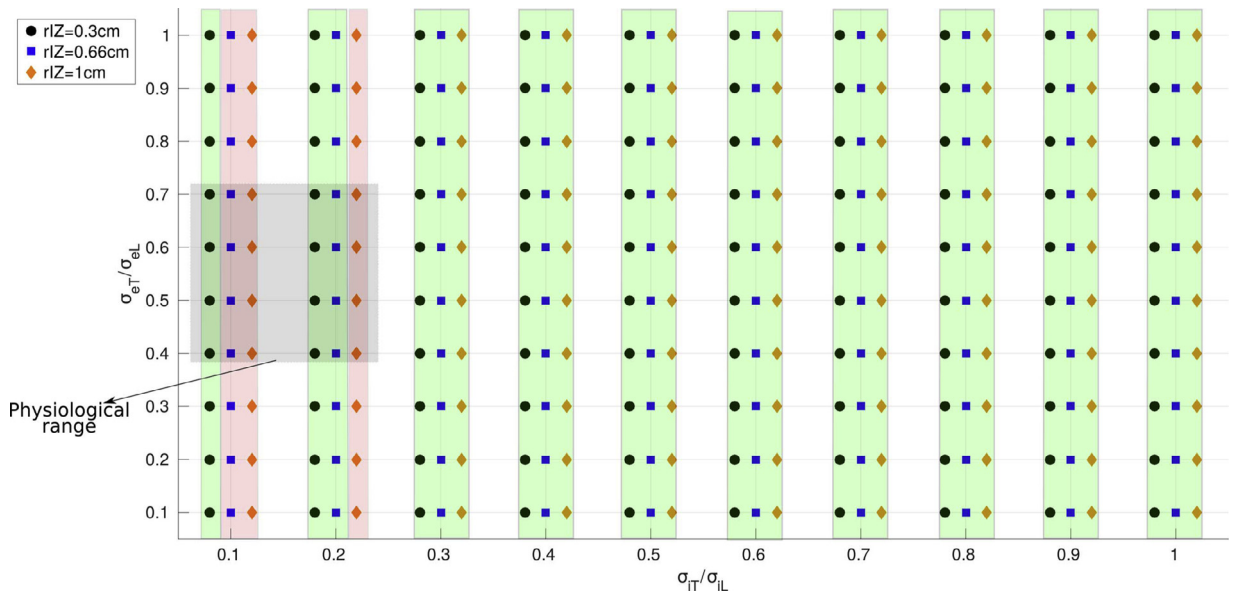


**Fig. 4.** Effects of changes in the intracellular and extracellular spaces at different rIZs. The green shading highlights spontaneous termination of reentrant activity. The red shading indicates spiral maintenance and pinning to the heterogeneity. The gray shading emphasizes the physiological range of the ratio  $\sigma_{IT}/\sigma_{IL}$  reported in the literature. (For interpretation of the references to color in this figure legend, the reader is referred to the web version of this article.)

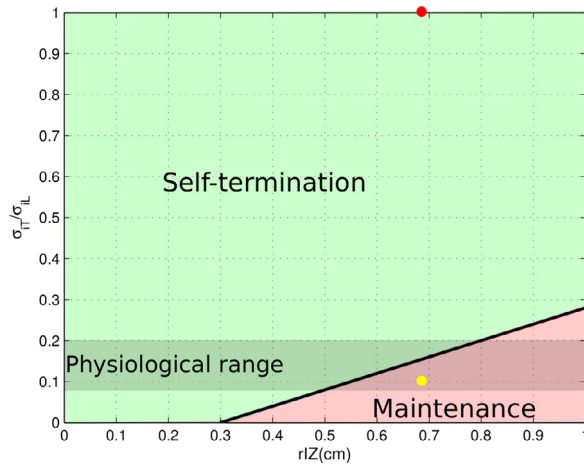


**Fig. 5.** Parameter space spanned by the radius rIZ of the ischemic region and the ratio  $\sigma_{IT}/\sigma_{IL}$  of the transversal and longitudinal intracellular conductivities characterizing electrical anisotropy. In the green area pinned spiral waves appear only during a transient phase and finally disappear due to self-termination. In the red area, instead, they are stable and persistent. The gray shading highlights the physiological range of the ratio  $\sigma_{IT}/\sigma_{IL}$  reported in the literature. The yellow and the red dots indicate parameters used for simulations shown in Figs. 1 and 2, respectively. In Fig. 1  $\sigma_{eT} = 40\% \sigma_{eL}$ , in Fig. 2  $\sigma_{eT} = \sigma_{eL}$  for comparison with ideal isotropic conditions. (For interpretation of the references to color in this figure legend, the reader is referred to the web version of this article.)

longitudinal ones. The green shading on the graph highlights conditions in which reentrant activity spontaneously terminates. The red shading indicates combinations of parameters that allow the system to maintain the spiral stable, pinned to the heterogeneity. The gray shading emphasizes the physiological range of the ratio  $\sigma_{IT}/\sigma_{IL}$  and the ratio  $\sigma_{eT}/\sigma_{eL}$  reported in the literature [32–36].

For all sizes of the heterogeneity, the outcome of the simulations seems not to be significantly affected by a variation of the extracellular conductivities, i.e. only quantitative changes of the dynamic behavior of the waves are observed, but not a transition between self-termination and maintenance. The major role in this context is played, instead, by the intracellular parameters, as it becomes more clear from the results shown in Fig. 5.

Fig. 5 focuses on IZ dimensions and intracellular anisotropy, once established that extracellular conductivities are not decisive parameters for determining the system evolution. Combinations of parameters are collected into two groups and highlighted in red in case of spiral maintenance and green in case of spiral self-termination. Once again, the gray shading emphasizes the physiological range of the ratio  $\sigma_{IT}/\sigma_{IL}$  reported in the literature [32–36]. As it was already observed in

Fig. 4, no difference is shown for small heterogeneities, until a threshold for the IZ dimension is reached. This threshold consists of a radius  $r_{IZ}$  of approximately 0.3 cm, beyond that increasing the radius  $r_{IZ}$  seems to promote the occurrence of reentrant activity maintenance over self-termination for high intracellular anisotropy (lower part of the graph). In particular, for the same radius  $r_{IZ}$ , getting closer to isotropic conditions promotes instead the transition from maintenance to self-termination. This tendency becomes progressively stronger the more the heterogeneity is extended.

The examples shown in Figs. 1 and 2 are marked, respectively, by the yellow and the red dots in Fig. 5.

In Fig. 1 extracellular and intracellular parameters are set in order to have  $\sigma_{iT} = 10\%\sigma_{iL}$  and  $\sigma_{eT} = 40\%\sigma_{eL}$ , a combination of parameters that is pretty close to what is found in literature [32] and that reproduces realistic conditions of tissue anisotropy. Simulations are run for a sufficiently long interval that allows to evaluate the spiral maintenance.

In Fig. 2 ideal conditions of isotropy are imposed in both extracellular and intracellular domains, i.e.  $\sigma_{iT} = \sigma_{iL}$  and  $\sigma_{eT} = \sigma_{eL}$ . This corresponds to an absence of fibers that causes the conduction velocity to be the same in the whole tissue without any directionality effect. The pinned spiral rotates then much faster than in Fig. 1 and the tip of the spiral collides with its tail (Fig. 2(c)). As a consequence the wave slowly annihilates itself and extinguishes, leading to spontaneous termination of electrical activity (Fig. 2(f)).

Different conductivities play a fundamental role in this process and can affect the outcome. In Fig. 1 there is a different conduction velocity imposed by fibers in parallel and perpendicular directions. This causes the wave to be sufficiently “slowed down” and, since  $r_{IZ}$  is extended enough, the period of the spiral is also long enough not to have any tip-tail collision. Thus, as a general statement, a high degree of intracellular anisotropy is more likely to induce maintenance of the spiral, depending on the size of the heterogeneity. However, this claim does not hold for too small heterogeneities (in which  $r_{IZ}$  is smaller than the threshold), where the period of the spiral is anyway too short.

## 5. Discussion

In this study, we used computer simulations of a 2D myocardium to investigate the role played by both geometry and conduction properties of the tissue in cardiac dynamics. In particular, we focused on the evolution of reentrant activity during acute ischemia and on how the size of the ischemic heterogeneity, together with the degree of tissue anisotropy, can contribute to maintenance or self-termination of pinned spirals. The use of the bidomain formulation allowed on one side to separate the effects of changes in intracellular and extracellular conductivities and, on the other side, to make a direct comparison between several anisotropic and totally isotropic conditions.

The main results of this study are:

- for the stability of the waves, changes of conductivity in the intracellular space are more critical than alterations in the extracellular space;
- the maintenance or the self-termination of pinned spirals is strongly dependent not only on the size of the heterogeneities but also on the degree of intracellular anisotropy.

As shown in our simulations, if the size of the ischemic heterogeneity is kept fixed above a certain threshold, intracellular conductivities are the most affecting parameters, able to strongly determine the evolution of the wave dynamics towards spiral maintenance or self-termination. A change in the extracellular space, instead, can cause only minor effects on the conductive behavior. This finding is in good agreement with Fry et al. [40], who showed experimentally that abnormalities in cellular action potentials during cardiac hypertrophy are mostly due to changes in coupling via gap junctions, regulated by intracellular conductivities. Our study, then, confirmed and extended this finding to the case of reentrant activity and acute ischemia, showing how intracellular conductivities still remain the “leading parameters” in case of dynamical instabilities and reentries during cardiac arrhythmias.

As previously said, although experiments to measure conductivities have been made, their results are inconsistent and no consensus exists regarding the conductivity values and their anisotropy ratios. For this reason, we decided to extend the analysis to a wider range of degrees of anisotropy, as it is shown in Figs. 4 and 5. Therefore, some of the combinations of parameters presented do not fit “discordant experimental data” published so far, in which the ratio  $\sigma_{iT}/\sigma_{iL}$  falls in the range between 8% and 20% and the ratio  $\sigma_{eT}/\sigma_{eL}$  falls in the range between 40% and 70%. Nevertheless, this approach allowed us to compare results obtained from realistic anisotropic and ideal isotropic conditions, as shown in Fig. 5.

Fig. 5 summarizes the simulation results highlighting the role played by the size of the heterogeneity, in combination with the degree of intracellular anisotropy. It is already known from previous investigations that a *sufficiently large obstacle in a tissue tends to make reentry more stable* [23] and that in the presence of a “hole” dynamical instabilities like spiral breakup transients can evolve either into stable reentry or quiescence depending on the radius  $r_{IZ}$  and its critical size [24]. In our simulations, the “hole” is an ischemic heterogeneity made up of real tissue following proper electrophysiological dynamics and having reduced conduction properties, i.e. playing an active role in the global simulation. Therefore, this study allows to evaluate the spontaneous termination of spirals including both normal and pathological dynamics. In the physiological range of Fig. 5 (lower part of the graph, between 8% and 20%) if  $r_{IZ}$  is greater than the threshold ( $r_{IZ} \simeq 0.3$  cm) the value of  $\sigma_{iT}/\sigma_{iL}$  is crucial for determining the system’s behavior, even for the same size of the heterogeneity, as it has been previously discussed in Section 3. This observation suggests that for the analysis of spontaneous termination of waves not only the radius of the ischemic zone  $r_{IZ}$  but also anisotropy has to be taken into account: underestimating it or supposing absence of fibers can lead in fact to completely different and misleading results, as shown in the comparison

between Figs. 1 and 2. Translated into clinical practice, the level of intercellular coupling is controlled through the major cardiac gap junction protein, connexin43 (Cx43), which during acute ischemia undergoes a process of loss of phosphorylation [41]. Specific drugs targeted to control connexin phosphorylation represent a way to actively intervene on the expression levels of connexins [42] and a model able to link intracellular anisotropy to other quantities (like  $\rho IZ$ ) may be a useful tool to investigate and promote self-termination of reentrant activity.

## 6. Conclusion

We have shown that the evolution of reentrant activity towards spontaneous termination or maintenance of spiral waves can be highly affected by heart conductivity, in particular by the degree of anisotropy of the tissue. The implementation of a bidomain model allowed us to focus on the role played by conductivity tensors in both the intracellular and the extracellular spaces under acute ischemic conditions: results from our simulations highlighted the dominant role exerted on wave dynamics by changes in intracellular conductivities. In addition, we also analyzed these changes in relation to other parameters (i.e. size of the ischemic heterogeneities) in order to appreciate a more realistic dynamics. Although the analysis was performed only in 2D domains, the obtained results already support the hypothesis that in this context tissue anisotropy is a fundamental component that definitely cannot be neglected in order to avoid misleading results. In addition, since experimental values of conductivity tensors known from literature are not consistent, this kind of analysis can be useful to get an overview of possible scenarios arising from a broader range of supposed anisotropy values. Therefore, although being preliminary, these results clearly indicate that the degree of anisotropy should be included in the list of parameters that play a key role in terminating arrhythmias.

## Acknowledgment

The research leading to the results has received funding from the [Deutsche Forschungsgemeinschaft \(SFB 1002, project C03\)](#) and German Center for Cardiovascular Research (DZHK), partnersite Goettingen.

## References

- [1] Iwasaki Y, Nishida K, Kato T, Nattel S. Atrial fibrillation pathophysiology: implications for management. *Circulation* 2011;124:2264–74.
- [2] Cherry EM, Fenton F. Visualization of spiral and scroll waves in simulated and experimental cardiac tissue. *New J Phys* 2008;10:1–43.
- [3] Wit AL, Cranefield PF. Reentrant excitation as a cause of cardiac arrhythmias. *Am J Physiol Heart Circ Physiol* 1978;235:1–17.
- [4] Kirsten HW, Ten Tusscher J, Hren R, Panfilov AV. Organization of ventricular fibrillation in the human heart. *Circ Res* 2007;100:87–101.
- [5] Jalife J, Delmar M, Anumonwo J, Berenfeld O, Kalifa J. Basic cardiac electrophysiology for the clinician. Chichester, West Sussex, UK: John Wiley & Sons; 2009.
- [6] Cherry EM, Fenton FH, Gilmour RF Jr. Mechanisms of ventricular arrhythmias: a dynamical systems-based perspective. *Am J Physiol Heart Circ Physiol* 2012;302:2451–63.
- [7] Qu Z. Chaos in the genesis and maintenance of cardiac arrhythmias. *Prog Biophys Mol Biol* 2011;105:247–57.
- [8] Chen PS, Wolf PD, Dixon EG, Danieley ND, Frazier DW, Smith WM, et al. Mechanism of ventricular vulnerability to single premature stimuli in open-chest dogs. *Circ Res* 1988;61:1191–209.
- [9] Winfree AT. Sudden cardiac death: a problem in topology. *Sci Am* 1983;248:144–9.
- [10] Cao JM, Qu Z, Kim YH, Wu TJ, Garfinkel A, Weiss JN, et al. Spatiotemporal heterogeneity in the induction of ventricular fibrillation by rapid pacing: importance of cardiac restitution properties. *Circ Res* 1999;84:1318–31.
- [11] Pastore JM, Girouard SD, Laurita KR, Akar FG, Rosenbaum DS. Mechanism linking t-wave alternans to the genesis of cardiac fibrillation. *Circulation* 1999;99:1385–94.
- [12] Qu Z, Garfinkel A, Chen PS, Weiss JN. Mechanisms of discordant alternans and induction of reentry in simulated cardiac tissue. *Circulation* 2000;102:1664–70.
- [13] Weiss JN, Karma A, Shiferaw Y, Chen PS, Garfinkel A, Qu Z. From pulsus to pulseless: the saga of cardiac alternans. *Circ Res* 2006;98:1244–53.
- [14] Otani NF. Theory of action potential wave block at-a-distance in the heart. *Phys Rev E* 2007;75:021910.
- [15] Comtois P, Vinet A, Nattel S. Wave block formation in homogeneous excitable media following premature excitations: dependence on restitution relations. *Phys Rev E* 2005;72: 031919.
- [16] Wiener N, Rosenblueth A. The mathematical formulation of the problem of conduction of impulses in a network of connected excitable elements, specifically in cardiac muscle. *Arch Inst Cardiol Mex* 1946;16:205–65.
- [17] Jalife J, Berenfeld O, Mansour M. Mother rotors and fibrillatory conduction: a mechanism of atrial fibrillation. *Cardiovasc Res* 2002;54:204–16.
- [18] Chen PS, Wu TJ, Ting CT, Karagueuzian HS, Garfinkel A, Lin SF, et al. A tale of two fibrillations. *Circulation* 2003;108:2298–303.
- [19] Moe GK. On the multiple wavelet hypothesis of atrial fibrillation. *Arch Int Pharmacodyn Ther* 1982;14:183–8.
- [20] Garrey W. The nature of fibrillary contraction of the heart – its relation to tissue mass and form. *Am J Physiol* 1914;33:397–414.
- [21] Bragard J, Simic A, Elorza J, Grigoriev RO, Cherry EM, Gilmour RF Jr, et al. Shock-induced termination of reentrant cardiac arrhythmias: comparing monophasic and biphasic shock protocols. *Chaos* 2013;23(4):043119.
- [22] Leon LJ, Roberge FA, Vinet A. Simulation of two-dimensional anisotropic cardiac reentry: effects of the wavelength on the reentry characteristics. *Ann Biomed Eng* 1994;22:592–609.
- [23] Xie F, Qu Z, Garfinkel A. Dynamics of reentry around a circular obstacle in cardiac tissue. *Phys Rev E* 1998;58:6355–8.
- [24] Qu Z. Critical mass hypothesis revisited: role of dynamical wave stability in spontaneous termination of cardiac fibrillation. *Am J Physiol Heart Circ Physiol* 2006;290:255–63.
- [25] Azene EM, Trayanova NA, Warman E. Wave front-obstacle interactions in cardiac tissue: a computational study. *Ann Biomed Eng* 2001;29:35–46.
- [26] Luo C, Rudy Y. A model of the ventricular cardiac action potential. Depolarization, repolarization, and their interaction. *Circ Res* 1991;68:1501–26.
- [27] Shaw RM, Rudy Y. Electrophysiologic effects of acute myocardial ischemia: a theoretical study of altered cell excitability and action potential duration. *Circ Res* 1997;35:256–72.
- [28] Bernus O, Zemlin CW, Zaritsky RM, Mironov SF, Pertsov AM. From pulsus to pulseless: the saga of cardiac alternans. *Europace* 2005;7:93–104.
- [29] Kléber AG, Riegger CB. Electrical constants of arterially perfused rabbit papillary muscle. *J Physiol* 1997;385:307–24.
- [30] Wilkswy JP Jr, Lin SF, Abbas RA. Virtual electrodes in cardiac tissue: a common mechanism for anodal and cathodal stimulation. *Biophys J* 1995;69:2195–210.
- [31] Larson C, Dragnev L, Trayanova N. Analysis of electrically induced reentrant circuits in a sheet of myocardium. *Ann Biomed Eng* 2003;31:768–80.

- [32] Clerc L. Directional differences of impulse spread in trabecular muscle from mammalian heart. *J Physiol* 1976;255:335–46.
- [33] Roberts D, Hersch LT, Scher AM. Influence of cardiac fiber orientation on wavefront voltage, conduction velocity, and tissue resistivity in the dog. *Circ Res* 1979;44:701–12.
- [34] Roberts D, Scher AM. Effect of tissue anisotropy on extracellular potential fields in canine myocardium in situ. *Circ Res* 1982;50:342–51.
- [35] Roth BJ. The electrical potential produced by a strand of cardiac muscle: a bidomain analysis. *Ann Biomed Eng* 1988;16:609–37.
- [36] Roth BJ. Non-sustained reentry following successive stimulation of cardiac tissue through a unipolar electrode. *J Cardiovasc Electrophysiol* 1997;8:768–78.
- [37] Sachse FB. Computational cardiology: modeling of anatomy, electrophysiology, and mechanics. Heidelberg: Springer Press; 2004.
- [38] Saffitz JE, Kléber AG. Gap junctions, slow conduction, and ventricular tachycardia after myocardial infarction. *J Am Coll Cardiol* 2012;60:1111–13.
- [39] Tranum-Jensen J, Janse MJ, Fiolet JWT, Krieger WJG, D'Alnoncourt CN, Durrer D. Tissue osmolality, cell swelling, and reperfusion in acute regional myocardial ischemia in the isolated porcine heart. *Circ Res* 1981;49:364–81.
- [40] Fry CH, Gray RP, Dhillon PS, Jabr RI, Dupont E, Patel PM, et al. Architectural correlates of myocardial conduction: changes to the topography of cellular coupling, intracellular conductance, and action potential propagation with hypertrophy in guinea-pig ventricular myocardium. *Circ Arrhythm Electrophysiol* 2014;7:1198–204.
- [41] Beardslee MA, Tadros PN, Schuessler RB, Kléber AG, Saffitz JE. Dephosphorylation and intra-cellular redistribution of ventricular connexin43 during electrical uncoupling induced by ischemia. *Circ Res* 2000;87:656–62.
- [42] Saffitz JE. Regulation of intercellular coupling in acute and chronic heart disease. *Braz J Med Biol Res* 2000;33:407–13.